

Light impurities in JET plasmas: transport mechanisms and effects on thermal transport

N. Bonanomi^{1,2}, P. Mantica², C. Giroud³, C. Angioni⁴, J. Citrin^{5,6}, E. Lerche⁷, P. Manas⁴, S. Menmuir³, C. Sozzi², M. Tsalas^{5,3}, D. Taylor³, D. Van Eester⁷ and JET contributors*

EUROfusion Consortium, JET, Culham Science Centre, Abingdon, OX14 3DB, UK

¹ Università di Milano-Bicocca, Milano, Italy

⁴ IPP-Garching Garching bei Munchen, Germany

⁷ LPP-ERM/KMS, TEC partner, 1000 Brussels, Belgium

² CNR - Istituto di Fisica del Plasma "P. Caldirola", Milano, Italy

⁵ FOM Institute DIFFER, 5600 HH, Eindhoven, The Netherlands

³ Culham Centre for Fusion Energy, Abingdon, OX14 3DB, UK

⁶ CEA, IRFM, F-13108 Saint Paul Lez Durance, France

* See the Appendix of F. Romanelli et al., Proceedings of the 25th IAEA Fusion Energy Conference 2014, Saint Petersburg, Russia

INTRODUCTION

A series of experiments was carried out in JET ILW L-mode plasmas in order to study the transport of light impurities and their effects on core thermal transport. These discharges feature the presence of ³He, Be, C, N, whose profiles are all measured by active Charge Exchange, although with different degrees of accuracy. To study the effects on ion heat transport, ICRH power was deposited on- and off-axis mainly to ions in (³He)-D minority scheme, in order to have a scan of the ion heat flux versus R/L_{Ti}, and also modulated for ion heat wave propagation. The density profiles of the light impurities in the plasma and the comparison with quasi-linear and non linear gyrokinetic simulations are shown. The impact on ions and electrons heat transport of the presence of nitrogen in the plasma is studied both analysing the experimental data and with gyrokinetic simulations.

LIGHT IMPURITY TRANSPORT

C-wall, L-mode plasmas. B₀ ~ 3.3 T, ICRH ~ 3-4 MW on- off-axis in (³He)-D minority scheme, NBI ~ 3 MW, I_p ~ 1.5 MA, n_{e,0} ~ 3 · 10¹⁹ m⁻³, T_{e,0} ~ 5 keV, T_{i,0} ~ 2.5 - 4 keV. Nitrogen puffed in discharges 86749/56/58 (N ~ 1.2%). N ~ 0% in discharges 86740/43/46.

Figure 3: Radial density profiles of ³He, Be, C and N. The density profiles of the same species are similar in all the discharges in which they are measured. The C profile is measured only for the discharge 86740 (N=0%), as the nitrogen has a big impact of the CX analysis of the C lines. The Plume effect is not considered for the ³He profile. The dashed purple lines are the profiles for a discharge with high rotation.

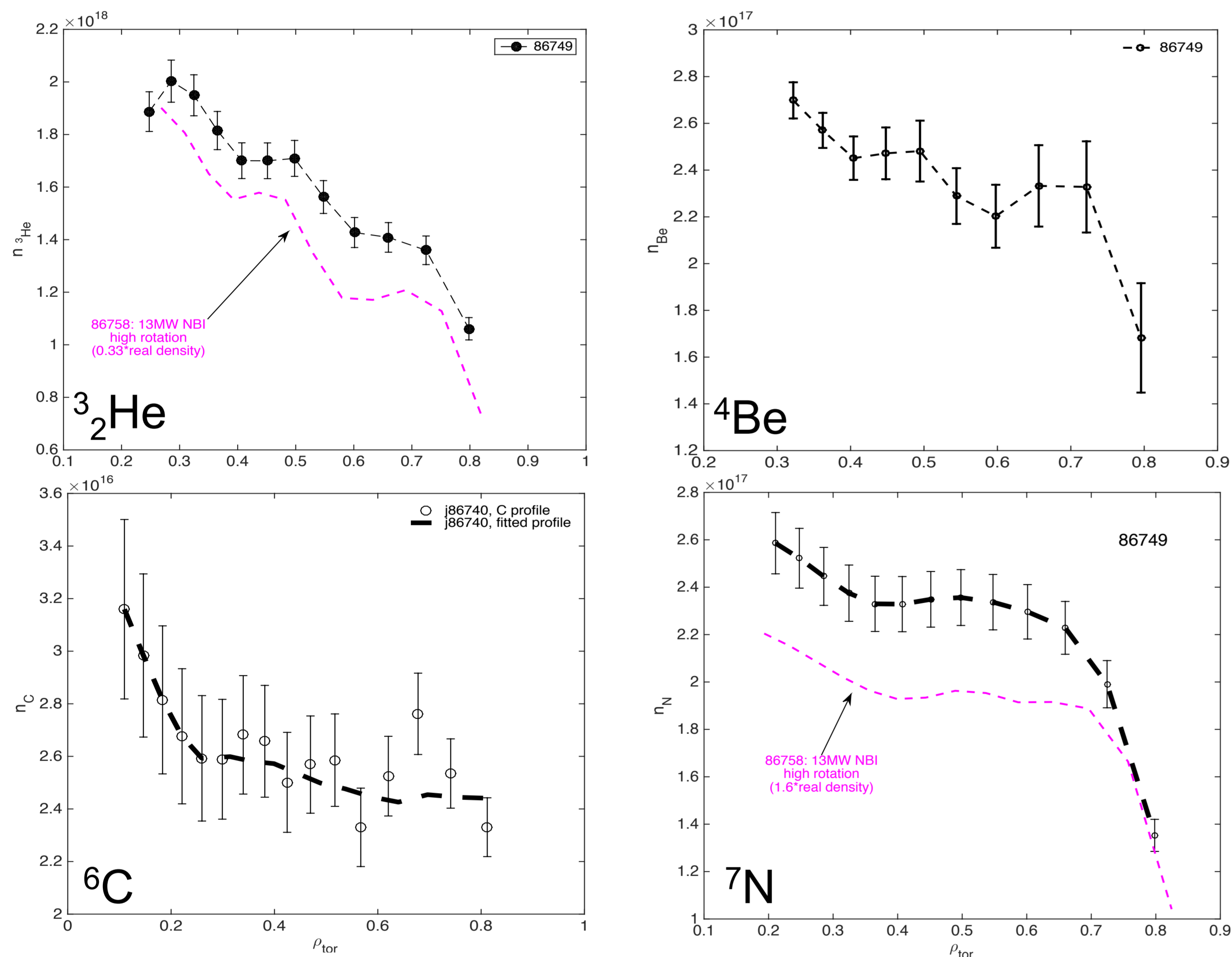
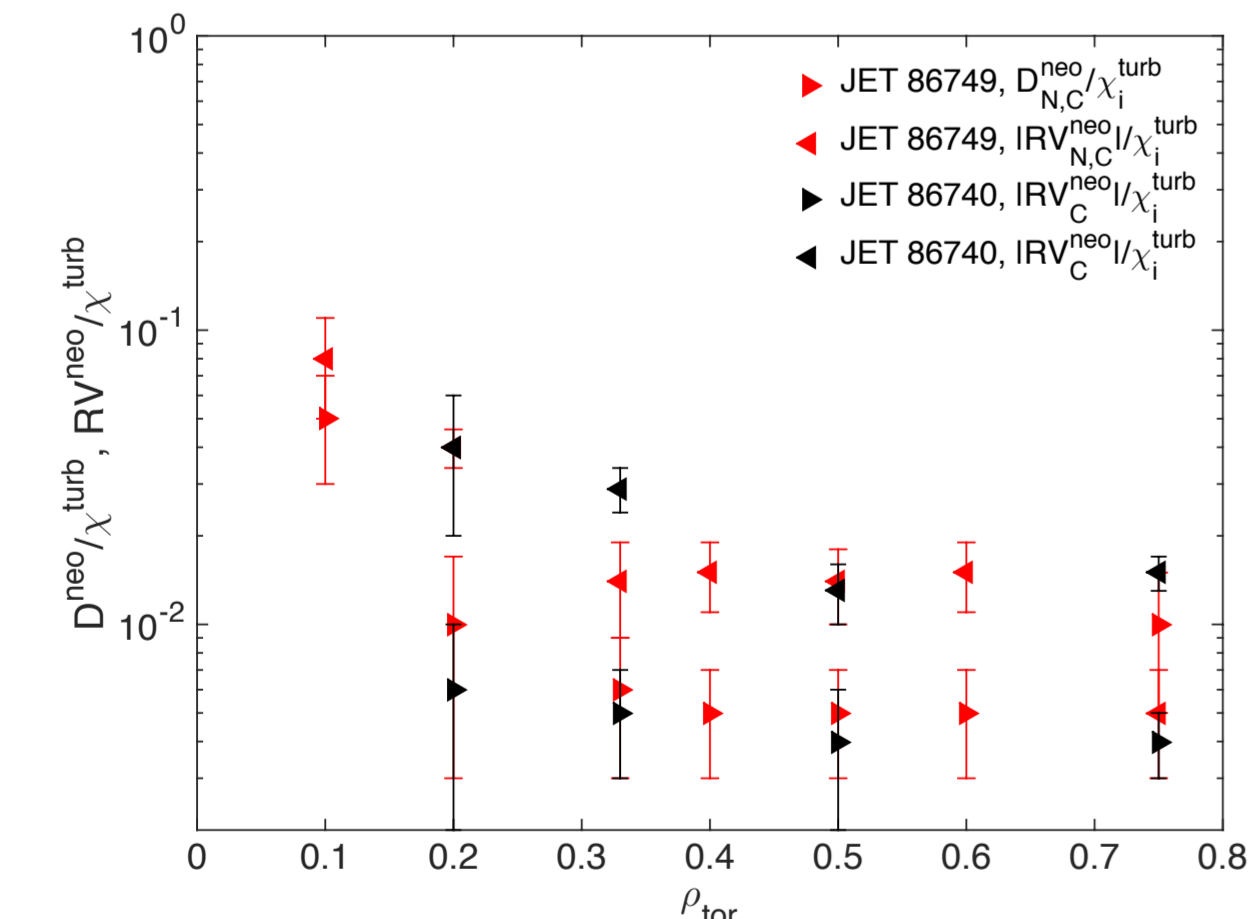


Figure 2: Neoclassical/turbulent contributions to the particle transport for N (red) and C (black). Left oriented triangles represent the convective part of the transport while right oriented triangles represent the diffusive part. The neoclassical contribution to the impurity particle transport is calculated with the NEO code [1] and results to be negligible, compared to the turbulent transport, outside $\rho_{tor} \sim 0.2$.



Contribution to the particle flux assuming no sources: C_T is the thermo-diffusion coefficient, C_R is the roto-diffusion coefficient and C_P is the pure pinch.

$$\frac{R}{L_{imp}} (\Gamma=0) = -\frac{RV}{D} = -\frac{D}{D} \left[C_T \cdot \frac{R}{L_{imp}} + C_R \cdot u' + C_P \right]$$

Table 1: Comparison between the experimental peaking of the impurities density profiles, the quasi-linear gyrokinetic simulations and with nonlinear gyrokinetic simulations (with GWK [2] and GENE [3]). The simulations underestimate the density peaking of the ³He and overestimate the peaking of ⁶C and ⁷N. The simulations indicate that important mechanisms [4] for the turbulent particle transport are the thermo-diffusion and the pure pinch, while the roto-diffusion is less important (~1/20 of the other terms).

		R/L _{imp} EXP	QL	NL
³ He	r= 0.33	2.5 +/- 0.5	1.25	/
	r= 0.5	2.8 +/- 0.5	0.7	/
⁴ Be	r= 0.5	peaked	0.7	/
⁶ C	r=0.2	2.5 +/- 0.5	/	/
	r= 0.5	0.3 +/- 0.5	1.3	1
⁷ N	r= 0.33	1.8 +/- 0.3	1.3	1.6
	r= 0.5	0.3 +/- 0.3	1.5	1-1.3

EFFECTS ON THERMAL TRANSPORT

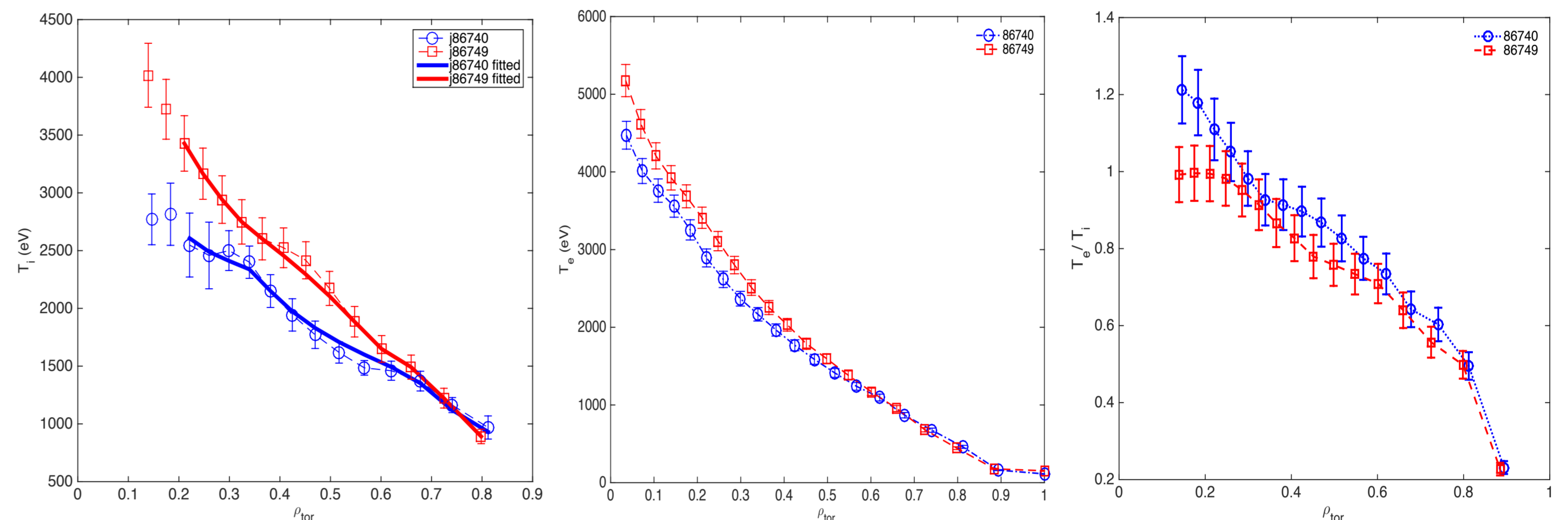


Figure 5: T_i radial profile (left), T_e profile (center) and T_e/T_i profile (right). Discharge 86740 (blue circles) representative of discharges without N. Discharge 86749 (red squares) representative of discharges with N.

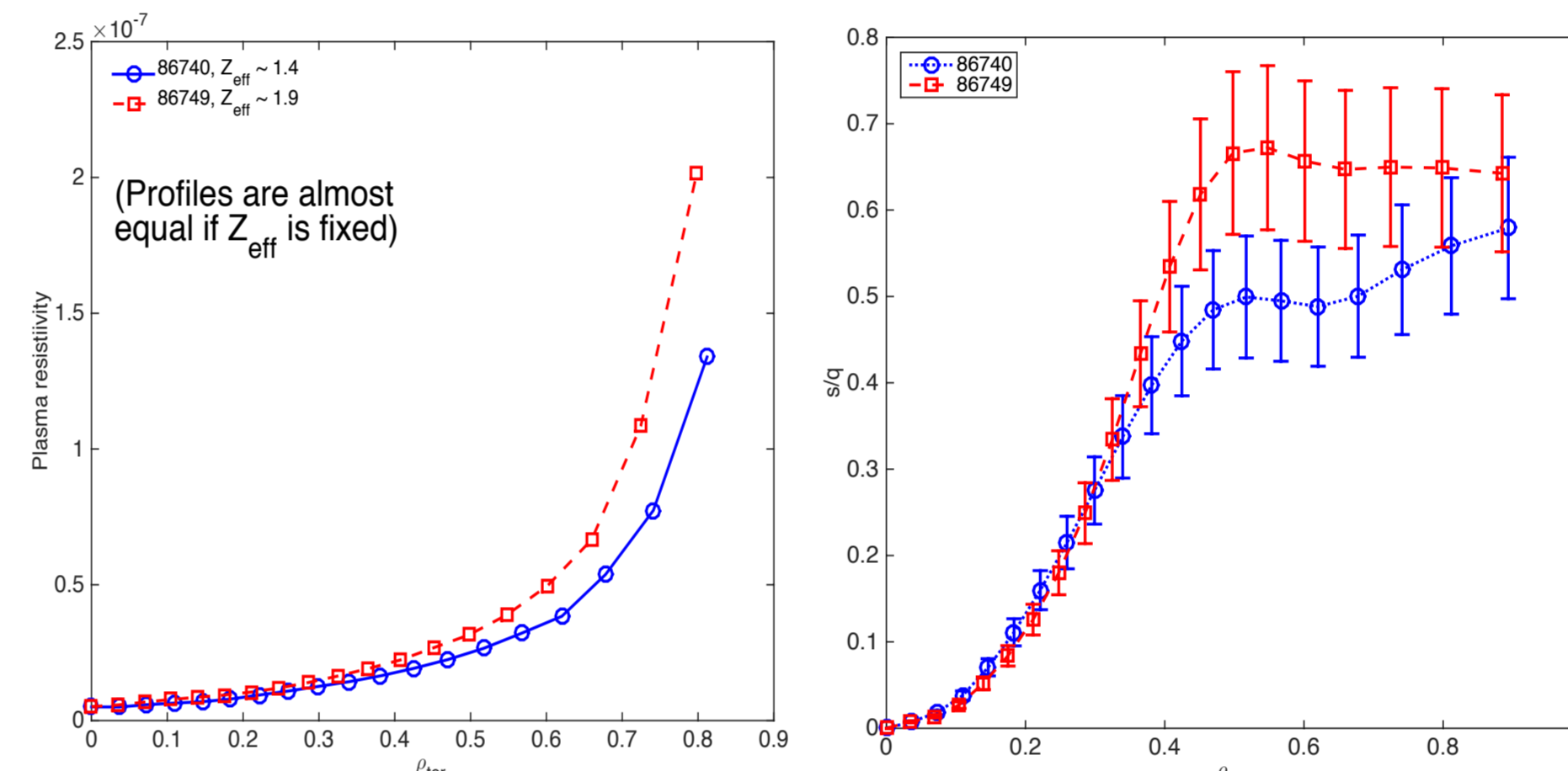


Figure 6: Radial profiles of plasma resistivity (left), and s/q (right) of discharges 86740 (blue circles, no N) and 86749 (red squares, N~1%). Difference in s/q can be a secondary effect of the N injection. Higher Z_{eff} causes higher plasma resistivity, that change the current density radial profile and so the q (and s) radial profiles.

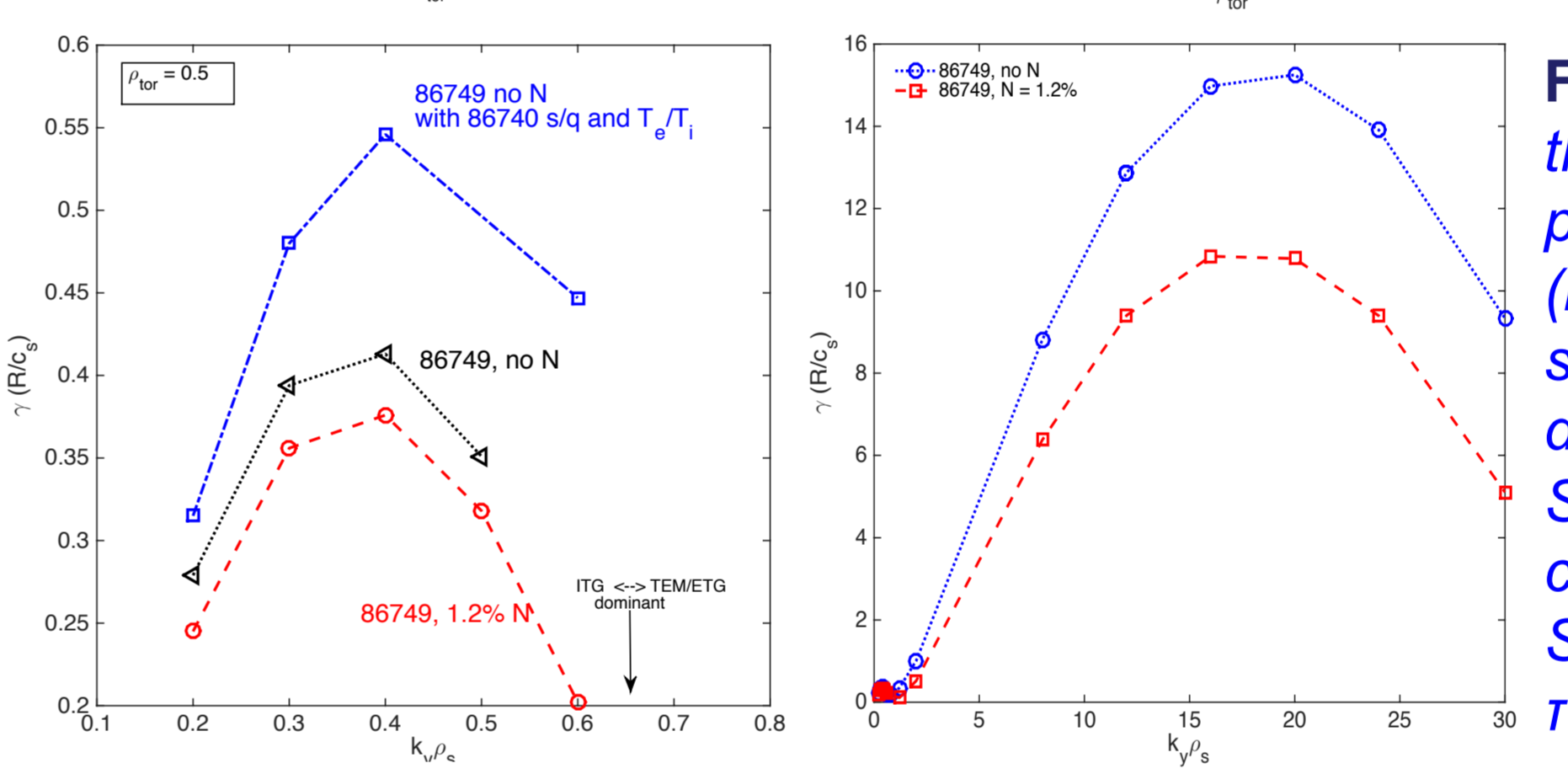


Figure 7: Linear gyrokinetic sim. of the effects of N, s/q and T_e/T_i on the plasma micro-instabilities on ion-scale (left) and electron-scale (right). The stabilization of ITG is due to main ion dilution and higher T_e/T_i and s/q [8,9]. Stabilization of TEM is due to higher collisionality and higher s [5,7]. Stabilization of ETG is due to higher $\tau = Z_{eff} T_e / T_i$.

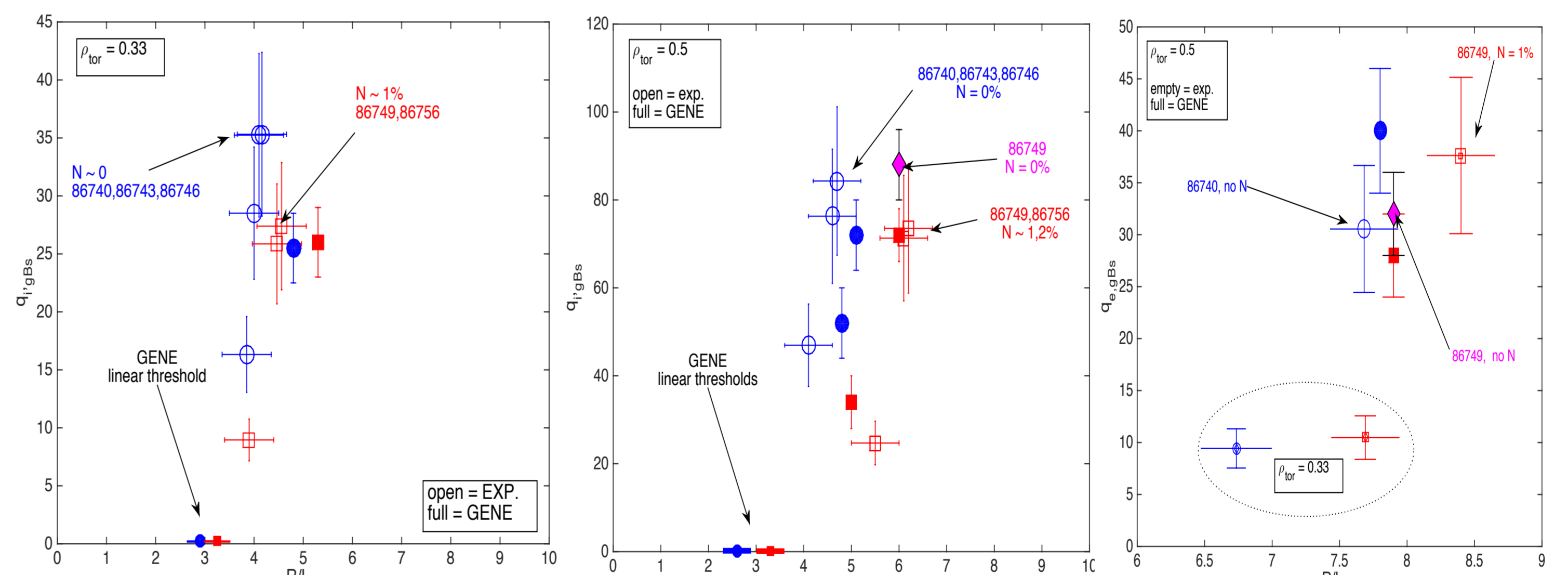


Figure 8: q_{i,GB} vs R/L_{Ti} (left and central) and q_{e,GB} vs R/L_{Te} (right). Open symbols=experimental points, full symbols=GENE non-linear simulations. The stabilization effects of N is visible at both radii, but is stronger at outer radii due to higher differences in s/q and T_e/T_i. The role of N is visible from the simulations (full purple diamond). On electrons, with N the values of R/L_{Te} are higher with the same flux.

CONCLUSIONS

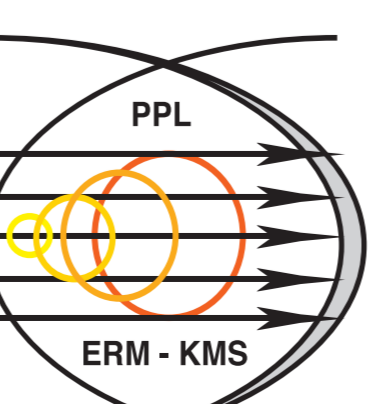
- Radial density profiles of four light impurities in a JET L-mode ILW discharge are shown.
- Known mechanisms for impurity transport in plasma are studied. The simulations underestimate the density peaking of the ³He and overestimate the peaking of ⁶C and ⁷N. The simulations indicate that the most important mechanisms for the turbulent transport are the thermo-diffusion and the pure pinch.
- The effect of the N on thermal transport is studied. The general effect is a stabilization of both the electron and the ion turbulent transport. The stabilization is due to different mechanisms, directly or indirectly caused by the presence of N.

ACKNOWLEDGMENTS

The authors would like to thank Yann Camenen for precious suggestions and discussions. This research used resources of the National Energy Research Scientific Computing Center, a DOE Office of Science User Facility supported by the Office of Science of the U.S. Department of Energy under Contract No. DE-AC02-05CH11231. A part of this work was carried out using the HELIOS supercomputer system at Computational Simulation Centre of International Fusion Energy Research Centre (IFERC-CSC), Aomori, Japan, under the Broader Approach collaboration between Euratom and Japan, implemented by Fusion for Energy and JAEA.

REFERENCES

- [1] E. Belli and J. Candy, Plasma Phys. Control. Fusion 50, 2008.
- [2] A.G. Peeters et al., Computer Physics Communications 180, 2009.
- [3] F. Jenko et al., Phys. Plasmas 7, 2000.
- [4] C. Angioni et al., Nucl. Fusion 52, 2012
- [5] F. Rytter et al., Phys. Rev. Letter 95, 2005
- [6] F. Jenko et al., Phys. Plasmas 8, 2001
- [7] N. Bonanomi et al., Nucl. Fusion 55, 2015
- [8] F. Romanelli, Phys. Fluids B 15, 1989.
- [9] P. Migliano et al., Plasma Phys. Control. Fusion 55, 2013



This work has been carried out within the framework of the EUROfusion Consortium and has received funding from the Euratom research and training programme 2014-2018 under grant agreement No 633053. The views and opinions expressed herein do not necessarily reflect those of the European Commission.